Electronic Supplementary Material (ESI) for Nanoscale.

Supporting Information for:

The combination of endolysosomal escape and basolateral stimulation to overcome the difficulties of "easy uptake hard transcytosis' of ligand-modified nanoparticles in oral drug delivery

Yi Cui, Wei Shan, Rui Zhou, Min Liu, Lei Wu, Quan Guo, Yaxian Zheng, Jiawei Wu, Yuan Huang *

Key Laboratory of Drug Targeting and Drug Delivery System (Ministry of Education), West China School of Pharmacy, Sichuan University, No. 17, Block 3, Southern Renmin Road, Chengdu 610041, China

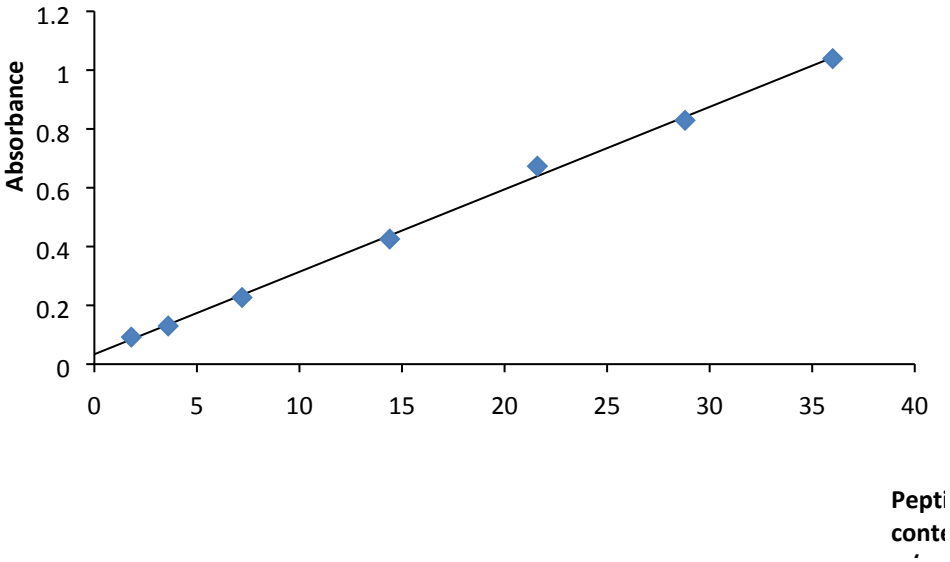

Supporting Information Figure S1. The calibration curve of peptide 22 measured by using the BCA protein assay reagent

Supporting Information Table S1. Determination of peptide-22 conjugation efficiency

The amount peptide detected by BCA (mg)	The amount of DSPE-PEG-peptide 22 conjugates (mg)	Conjugation efficiency (%)
8.75	31.8	27.5
12.6	47.1	26.8
16.3	58.9	28.1
The mean conjugation efficiency (%)		27.5 ± 0.65

Note: The peptide-22 conjugation efficiency was calculated as follows: Conjugation efficiency = (the amount peptide 22 detected by BCA/the amount of DSPE-PEG-peptide 22 conjugates) $\times$ 100

Supporting Information Table S2. Chemicals used to study the intracellular transport of nanocarriers

Chemicals	Function	Mechanism	Concentration
Peptide 22	Competitive inhibitior	Ligand for LDL, excessive existence could compete with other ligands for the binding with LDLR	2 mg/mL
LDL	Competitive inhibitior	Ligand for LDLR excessive existence would compete with other ligands for the binding with LDLR	100 μg/mL
Cholesterol	Competitive inhibitior	Mainly transported through LDLR pathway and excessive existence would compete with other ligands for the binding with LDLR	80μg/mL

Heparin	Receptor binding blocker	Inhibiting ligands to interact with LDLR	10 μg/mL
Chlorpromazine	Inhibits clathrin-mediated pathway	Rho GTPase inhibition	30 μM
Hypertonic sucrose	Inhibits clathrin-mediated pathway	The dispersion of clathrin lattices on the plasma membrane	0.4 M
Filipin	Inhibits caveolae -mediated pathway	Interacting with cholesterol	500 nM
Lovastatin	Inhibits caveolae -mediated pathway	Reversible inhibitors of the 3-hydroxy-3-methylglutaryl coenzyme A (HMG-CoA) reductase	10 μg/mL
Amiloride	Inhibits macropinocytosis	Lowering submembraneous pH and preventing Rac1 and Cdc42 signaling	12 μg/mL
Rottlerin	Inhibits macropinocytosis	Inhibiting either phosphoinositide 3-kinase (PI3K) or phosphoinositide-specific PLC	10 μM
Chloroquine	Lysosome-releasing activity	pH buffering capacity which prevented the activity of lysosomal enzymes	100 μM
Hemagglutinin-2 (HA_2)	Endosome-releasing activity	Interacting with endosomal membranes and cause a conformational change to a helical structure which resulted in escape outside of endosomal compartments	100 μM
Metformin	The regulation of constitutive exocytosis of lipoproteins	Activitor of 5′-AMP-activated kinase (AMPK)	1 mM
AICAR	The regulation of constitutive exocytosis of lipoproteins.	Activitor of 5′-AMP-activated kinase (AMPK)	0.5 mM

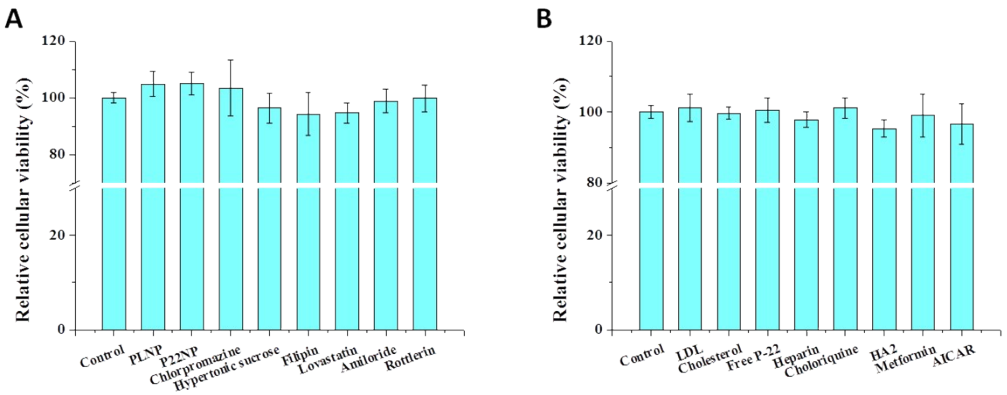

Supporting Information Figure S2. Cell viability after incubation of NPs or tested chemicals in Table S2. The concentration of PLNP and P22NP were selected based on previous study (600 μg/mL, PLGA concentration). The cells incubated with Hank's balanced salt solution (HBSS) were employed as a negative control and normalized for 100% cell viability. Data are means ± SD (n=3)

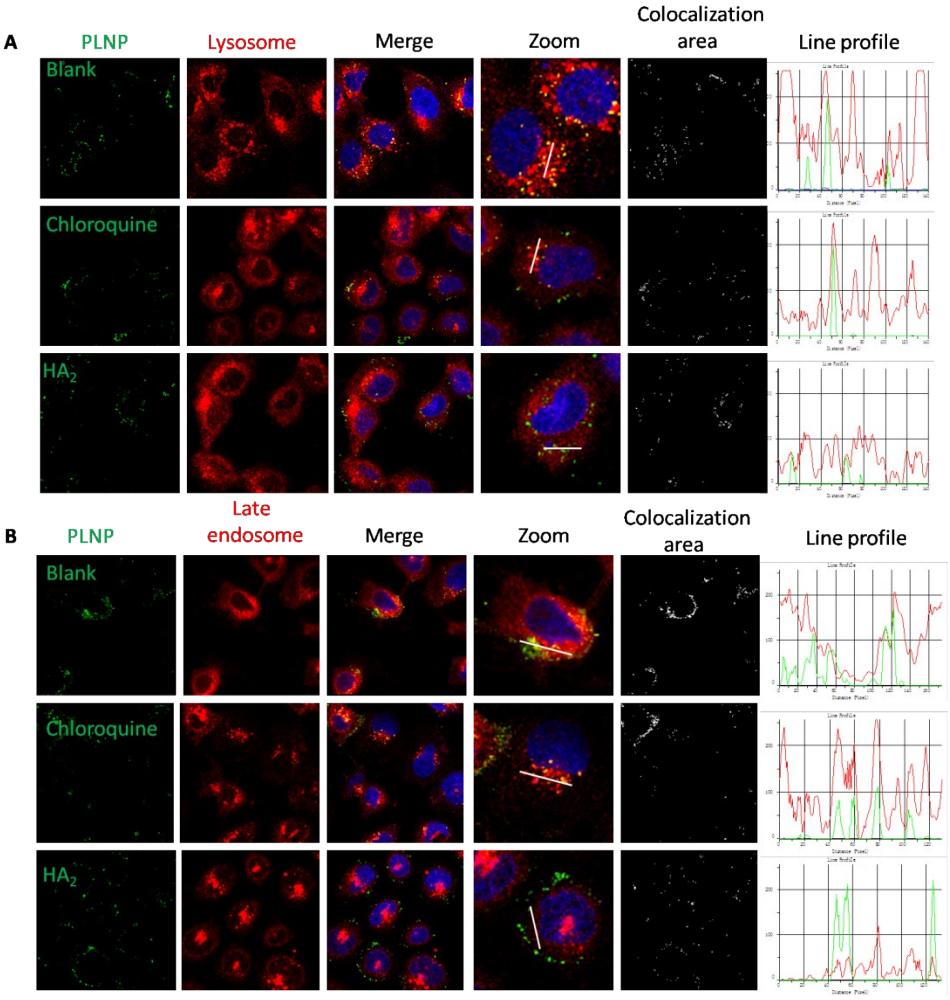

Supporting Information Figure S3. (A) & (B) The representative CLSM images of PLNP colocalized with lysosome and late endosome after NPs incubation with the presence of HBSS, chloruquine and HA_2, respectively. The colalization values and line profiles of PLNP were also illustrated.

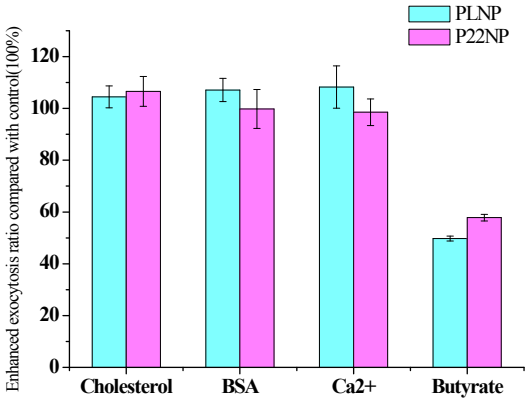

Supporting Information Figure S4. The effect of chemicals on the exocytosis of NPs (mean ± S.D., n = 3). In terms of BSA, Ca^{2+} and butyrate groups, the HBSS buffer was additionally containing bovine serum albumin (1% (v/v)), calcium ion (20 μM) or butyrate (2 mM).

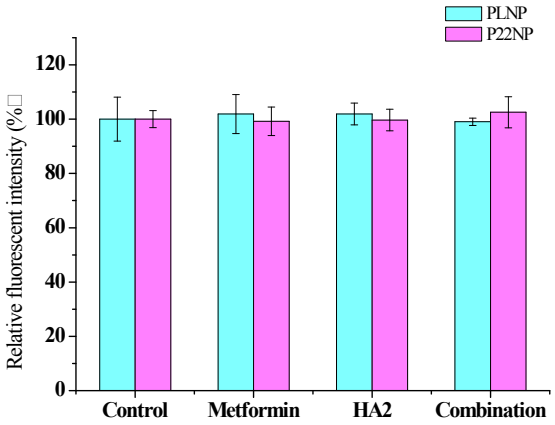

Supporting Information Figure S5. The effects of metformin and HA_2 on the endocytosis of P22NP or PLNP (mean ± S.D., n = 3).

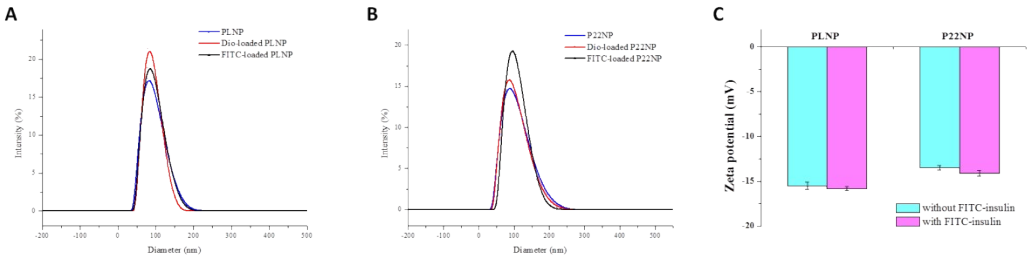

Supporting Information Figure S6. (A) & (B) The characterization of particles sizes detected by Malvern Zeta size NanoZS90 for PLNP and P22NP, respectively. When both of them loaded with FITC-labeled insulin, there was no significant influence on particle sizes. (C) Zeta potentials detected in distilled water (25 °C, pH 7.0). When P22NP or PLNP loaded with FITC-labeled insulin, there was no significant influence on Zeta potentials.